© 2017. Published by The Company of Biologists Ltd | Journal of Experimental Biology (2017) 220, 4644-4653 doi:10.1242/jeb.164343

RESEARCH ARTICLE

A new method to characterize function of the *Drosophila* heart by means of optical flow

Hauke Mönck[1], David Toppe[1], Eva Michael[2], Stephan Sigrist[2], Vincent Richter[1], Diana Hilpert[1], Davide Raccuglia[3], Marina Efetova[1] and Martin Schwärzel[1,*]

ABSTRACT

The minuteness of *Drosophila* poses a challenge to quantify performance of its tubular heart and computer-aided analysis of its beating heart has evolved as a resilient compromise between instrumental costs and data robustness. Here, we introduce an optical flow algorithm (OFA) that continuously registers coherent movement within videos of the beating *Drosophila* heart and uses this information to subscribe the time course of observation with characteristic phases of cardiac contraction or relaxation. We report that the OFA combines high discriminatory power with robustness to characterize the performance of the *Drosophila* tubular heart using indicators from human cardiology. We provide proof of this concept using the test bed of established cardiac conditions that include the effects of ageing, knockdown of the slow repolarizing potassium channel subunit KCNQ and ras-mediated hypertrophy of the heart tube. Together, this establishes the analysis of coherent movement as a suitable indicator of qualitative changes of the heart's beating characteristics, which improves the usefulness of *Drosophila* as a model of cardiac diseases.

KEY WORDS: Cardiovascular disease, Cardiovascular model, Cardiotropic effect, Adrenergic system, Octopamine

INTRODUCTION

Cardiovascular diseases are associated with a multitude of risk factors like diabetes, hypertension, obesity or smoking. Understanding of the underlying pathogenic principles is complicated by a complex interplay between lifestyle, genetic susceptibility and ageing (Yusuf et al., 2001). In order to elucidate this complex matter, large-scale clinical studies have been conducted in humans (e.g. Clerico et al., 2011; Gordon et al., 1977; Shah et al., 2012; Zheng et al., 2005) assisted by genetic screens in *Drosophila* that facilitated understanding of basic disease mechanisms (Gill et al., 2015; Neely et al., 2010; Olson et al., 2001; Ugur et al., 2016; Wolf et al., 2006). In contrast to its success as a genetic model system, the minuteness of *Drosophila* challenges the methods used to quantify performance of its tubular heart. Various approaches have been employed that include manual counting of heart vessel contractions (Zhu et al., 2016), electrophysiological recordings of muscle potential (Johnson et al., 1998) and sophisticated optical methods (Klassen et al., 2017; Wasserthal, 2007; Wolf et al., 2006). A resilient compromise between instrumental costs on the one hand and the richness in detail of the data on the other hand has been the semiautomatic optical heartbeat analysis (SOHA) developed by Fink and Ocorr, which determines functional parameters of the fly tubular heart from high-speed digital video film (Cammarato et al., 2015; Fink et al., 2009). Here, we present an extension of this method that utilizes an optical flow algorithm (OFA; Horn and Schunck, 1980; Lucas and Kanade, 1981) in order to extract cardiac movement from movies and uses this information in a twofold manner: firstly, to subscribe the time course of observation with the reiterating phases of cardiac contraction or relaxation, respectively; and secondly, to assign different movement qualities based on the magnitude and direction of the average vector of coherent movement.

MATERIALS AND METHODS

Fly care

Fly stocks were obtained from Bloomington Drosophila Stock Center (Bloomington, IN, USA) and from Vienna Drosophila Resource Center (Vienna, Austria). Flies were raised at either 25 or 30°C and 60% relative humidity with a 14 h:10 h light:dark cycle on cornmeal-based food following the Würzburg recipe (Guo et al., 1996). Genotypes containing UAS-RNAi constructs were raised at 30°C to improve efficacy of the knockdown. Genetic crosses were performed according to standard procedures. All experiments were performed with 5- to 7-day-old flies of both sexes unless otherwise indicated.

Compendium of fly lines

We used cantonized w^{1118} as the reference strain. We used the *Drosophila* GAL4-UAS system (Brand and Perrimon, 1993) to drive expression of various transgenes within the fly heart; we used Hand-Gal4 or tinC-Gal4 to drive expression within the cardiac vessel (Albrecht et al., 2006; Lo et al., 2002). We expressed either the voltage-sensitive dye UAS-arclight (Cao et al., 2013) or the photoactive adenylyl cyclase UAS-bPAC (Stierl et al., 2011). RNAi-mediated knockdown of either a KCNQ channel subunit or the ryanodine receptor was achieved by means of UAS-KCNQ-KD (VDRC ID 106655) or UAS-RyR-KD (VDRC ID 109631), respectively. We used the UAS-$Ras85D^{V12}$ transgene to induce cardiac hypertrophy (Yu et al., 2013).

Semi-intact preparation

We generated semi-intact preparations of the abdominal heart vessel as previously described (Fink et al., 2009; Ocorr et al., 2009). In brief, hearts were exposed by cutting off the head and ventral thorax followed by removal of the ventral abdominal cuticle and internal organs. Dissections were performed using artificial haemolymph containing 108 mmol l^{-1} $NaCl_2$, 5 mmol l^{-1} KCl, 2 mmol l^{-1} $CaCl_2$, 8 mmol l^{-1} $MgCl_2$, 1 mmol l^{-1} Hepes, 10 mmol l^{-1} sucrose and

[1]Freie Universität Berlin, Department of Biology/Neurobiology, Königin-Luise Strasse 28-30, D-14195 Berlin, Germany. [2]Freie Universität Berlin, Department of Biology/Neurogenetics, Takustrasse 6, D-14195 Berlin, Germany. [3]Institute of Neurophysiology, Charité - Universitätsmedizin, 10117 Berlin, Germany.

*Author for correspondence (martin.schwaerzel@fu-berlin.de)

M.S., 0000-0002-2071-1921

Received 9 June 2017; Accepted 9 October 2017

Journal of Experimental Biology

Journal of Experimental Biology (2017) 220, 4644-4653 doi:10.1242/jeb.164343

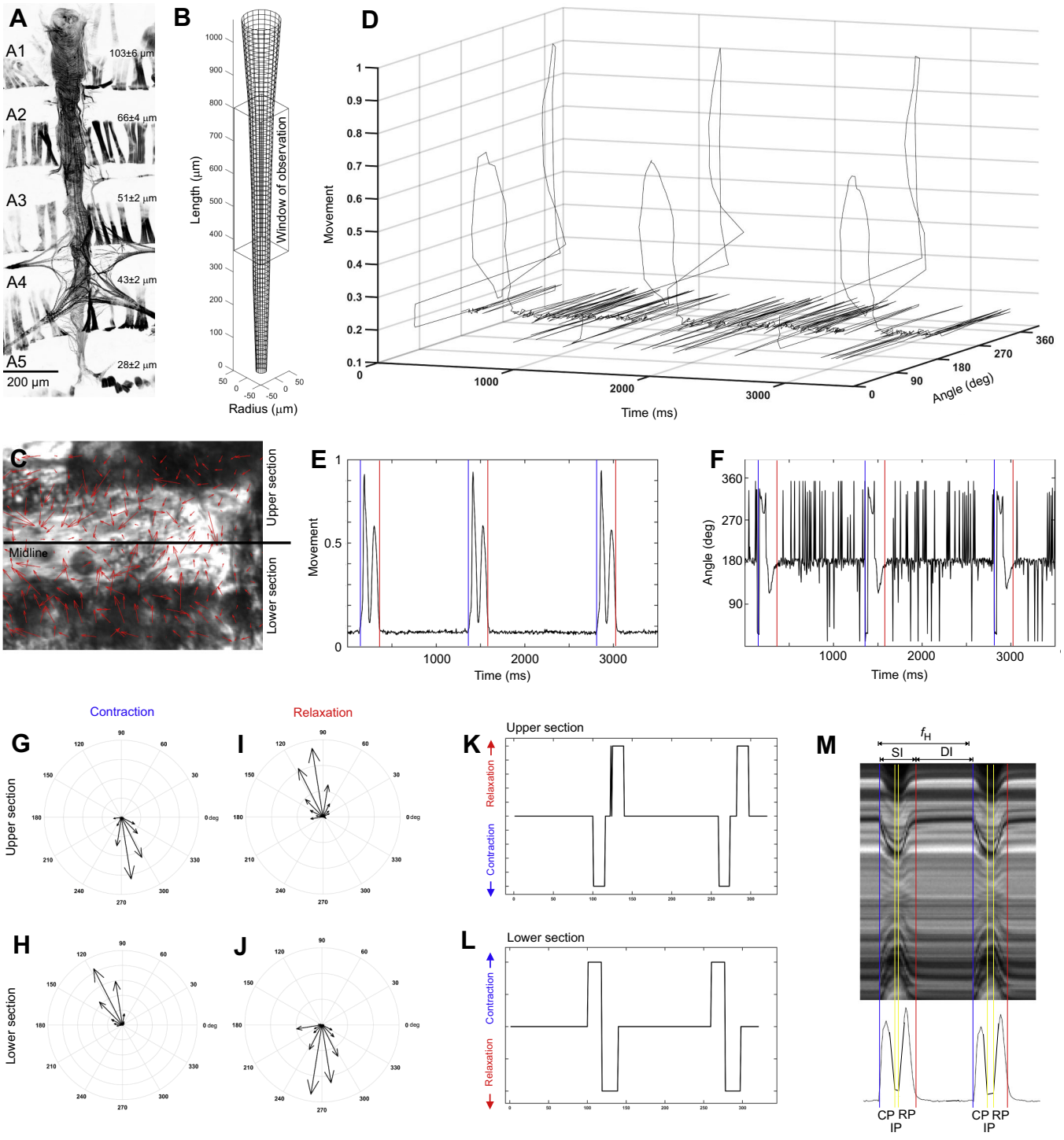

Fig. 1. See next page for legend.

5 mmol l^{-1} trehalose adjusted to pH 7.1. Dissections were performed at 25°C using a Leica M205C stereo dissecting microscope and recordings of heart activity were acquired at 25°C using an industrial camera (Basler piA640-210gm) mounted on a Nikon FN1 fixed-stage microscope equipped with a 10× water-immersion lens (Nikon). Frames were captured at 200 frames s^{-1} using TroublePix Software (NorPix Inc., Montreal, QC, Canada). Parameter extraction was done using an open source OFA running on a Matlab platform.

Calculation of optical flow

Optical flow (OF) was calculated using the Matlab estimateFlow function including Lucas–Kanade (Lucas and Kanade, 1981) and difference-of-gaussians methods. For each frame, we calculated the movement as the sum of all OF vector magnitudes per half-section and assigned orientation based on the direction. For interval detection, we calculated the overall direction likelihood per half-section and used the associated reverse section in the case of uncertain results. Interval detection inferred beats by semantically identifying segments of

Journal of Experimental Biology (2017) 220, 4644-4653 doi:10.1242/jeb.164343

Fig. 1. Functionality of the optical flow algorithm. The optical flow algorithm (OFA) provides direction and magnitude of movement for every pixel of a series of frames. We applied this method to high-speed videos of the exposed beating *Drosophila* heart to characterize performance of the fly's cardiac vessel. (A) Semi-intact preparation of the *Drosophila* heart contrasted with phalloidin to mark the muscle's actin filaments. Abdominal segments A1–A5 are visible as an alternating sequence of body wall musculature that horizontally spans the preparation. The heart tube spans the abdomen vertically with an inverted cone appearance and is fixed therein by segmentally arranged allary muscles that strike out within segment A4. The mean (±s.e.m., *N*=14 preparations) segmental diameter of the heart tube is indicated on the right-hand side. (B) 3D reconstruction of the *Drosophila* heart based on the segmental diameter and length data obtained from phalloidin-stained preparations yielded a vessel volume of 3.18±0.12 nl. The window of observation for digital videotaping is indicated and was used to determine velocity of the peristaltic wave that moves haemolymph along the longitudinal axis of the vessel. (C) The movement vectors determined by OFA are superimposed on a particular frame depicting the *Drosophila* heart. The midline represents a symmetry axis and separates the upper half from the lower half of the image. (D) Direction and relative magnitude of movement are plotted as a function of time. Note the prominent movement peaks. (E) Relative magnitude of movement as a function of time plotted in two dimensions omitting the directional aspect of movement. Onsets and offsets of movement are indicated by blue and red lines, respectively. Note the stereotyped bimodal movement pattern, which indicates contraction and relaxation of the systolic cycle. (F) Direction of movement as a function of time plotted in two dimensions omitting the magnitude aspect of movement. Note the stereotyped movement pattern during the movement phase, i.e. in between the blue and red lines, which is clearly separable from random movement during the rest phase that propagates from the red to the blue lines. (G–J) Direction and magnitude of movement during phases of contraction (G,H) or relaxation (I,J) of symmetric half-sections indicated in polar coordinates with the angle of the movement vector indicating the direction and its length indicating the magnitude of movement. (K,L) Movement extract for the upper (K) and lower (L) section as a function of time. Note the artifact within the upper section that we corrected based on data extracted from the lower section as we expect cardiac movement to be symmetrical to the vessel's longitudinal axis. (M) The M-mode is an established means to illustrate movement of the peristaltic wave along the longitudinal axis of the cardiac vessel for a particular pixel column (Fink et al., 2009). We superimposed the movement curve generated by the OFA and exemplified the particular phases of the systolic interval (SI), diastolic interval (DI) and heart rate (f_H) as deduced from the movement. Contraction phase (CP), isometric phase (IP) and relaxation phase (RP) were defined to further characterize the contractile movement of the heart vessel.

above-threshold contraction and relaxation directions. For radial plots, the per-frame main direction was determined by means of a gaussian fit. The source code is publicly available at https://github.com/hmoenck/OFAnalysis_supplementary.

Statistical analysis

Statistical analysis was done using Prism6 software (GraphPad Software Inc.).

Staining and confocal microscopy

Specimens were fixed in 4% paraformaldehyde (1 h at room temperature) followed by permeabilization in phosphate-buffered saline with Tween 20 (PBST; 30 min at room temperature) and staining with Phalloidin-Atto 550 (Sigma-Aldrich, St Louis, MO, USA) overnight (1/1000 dilution in PBS). Specimens were mounted in Vectorshield (Vectorlabs, Inc., Burlingame, CA, USA) and images were acquired using a Leica SP8 confocal laser scanning microscope. Image processing was done using ImageJ software.

RESULTS

The OFA yields magnitude and direction of contractile movement

The *Drosophila* tubular heart resides at the dorsal side of the abdomen and originates within abdominal segment 5 (A5) to propagate caudally until abdominal segment 1 (A1), where it passes over into the aorta (Fig. 1A). Confocal image stacks were used to create a scale model of the heart tube illustrating the image section seen by the camera that provides a basis for movement detection (Fig. 1B). The contractile movement of the tube was accessed by means of the OFA (Horn and Schunck, 1980; Lucas and Kanade, 1981), which detected the magnitude and direction of coherent movement in the video (Fig. 1C; Movie 1 illustrates coherent movement within a video of a wild-type heart tube). Given the symmetry of the heart to its longitudinal axis, we split the image into an upper and a lower section for separate evaluation. As a result, the OFA returned magnitude and direction of coherent movement at a temporal resolution of 5 ms (Fig. 1D) that could be collapsed to display either movement (Fig. 1E) or direction (Fig. 1F) separately. In contrast to the direction measure, the movement measure exhibited an excellent signal-to-noise ratio and allowed precise assignment of movement onset/offset that, in turn, could be allocated to appropriate directions based on the absolute time base. By this design, the OFA yielded continuous movement directions for the upper and lower sections (Fig. 1G–J) that we used to assign particular qualities, i.e. contraction or relaxation. Moreover, symmetry along the longitudinal axis allowed for an additional correction of processing errors (arrowhead in Fig. 1K,L) so that the OFA was able to subscribe the time line of the movie in a robust fashion (Fig. 1M). In detail, the algorithm assigned the reiterating phases of the systolic interval (SI) and the diastolic interval (DI) that together define the heart rate (f_H), as previously reported (Fink et al., 2009; Ocorr et al., 2009). As noted by Cammarato and colleagues (2015), the OFA provides a further subdivision of the contracted state by means of the additional measures contraction phase (CP), isometric phase (IP) and relaxation phase (RP), based on characteristic properties of the movement measure (Fig. 1M). The OFA provides a vector analysis method termed optical flow to evaluate *Drosophila* cardiac activity based on coherent movement.

Peristaltic movement along the heart's longitudinal axis

The tubular heart moves haemolymph by means of a peristaltic wave that propagates along its longitudinal axis (Fink et al., 2009). We accessed this movement by means of two image sections located at diametric ends of the image frame (Fig. 2A) to aid in detecting the absolute time basis of movement in particular sections separately (Fig. 2B,C). Delay time was determined by means of the sum-of-square difference algorithm (SSD; Fig. 2D) to provide a first approximation of axial movement. Next, we varied the width and distance of the image sections to yield optimal signal-to-noise ratios (Fig. 2E) and finally defined the velocity of the peristaltic wave along the longitudinal axis of the tubular heart for wild-type animals under resting conditions, i.e. 12.00±0.67 mm s^{-1}. In addition, the OFA yielded the global direction of longitudinal movement and revealed posterior to anterior as the preferred direction of movement in 79.6±1.8% of cases from a total of 401 wild-type preparations (Fig. 2F). Change of beat direction, i.e. heart beat reversal (Wasserthal, 2007), turned out to be a rare event in the case of the semi-intact heart preparation (Fig. 2G) that nevertheless was verifiable and augmented upon glutamatergic stimulation (t_{18}=3.13, P<0.05; Fig. 2H), as previously reported (Dulcis and Levine, 2005). Altogether, these results establish OFA as a sophisticated tool to extract global direction and speed of movement along the longitudinal axis from high-speed videos of semi-intact heart activity.

Journal of Experimental Biology

Journal of Experimental Biology (2017) 220, 4644-4653 doi:10.1242/jeb.164343

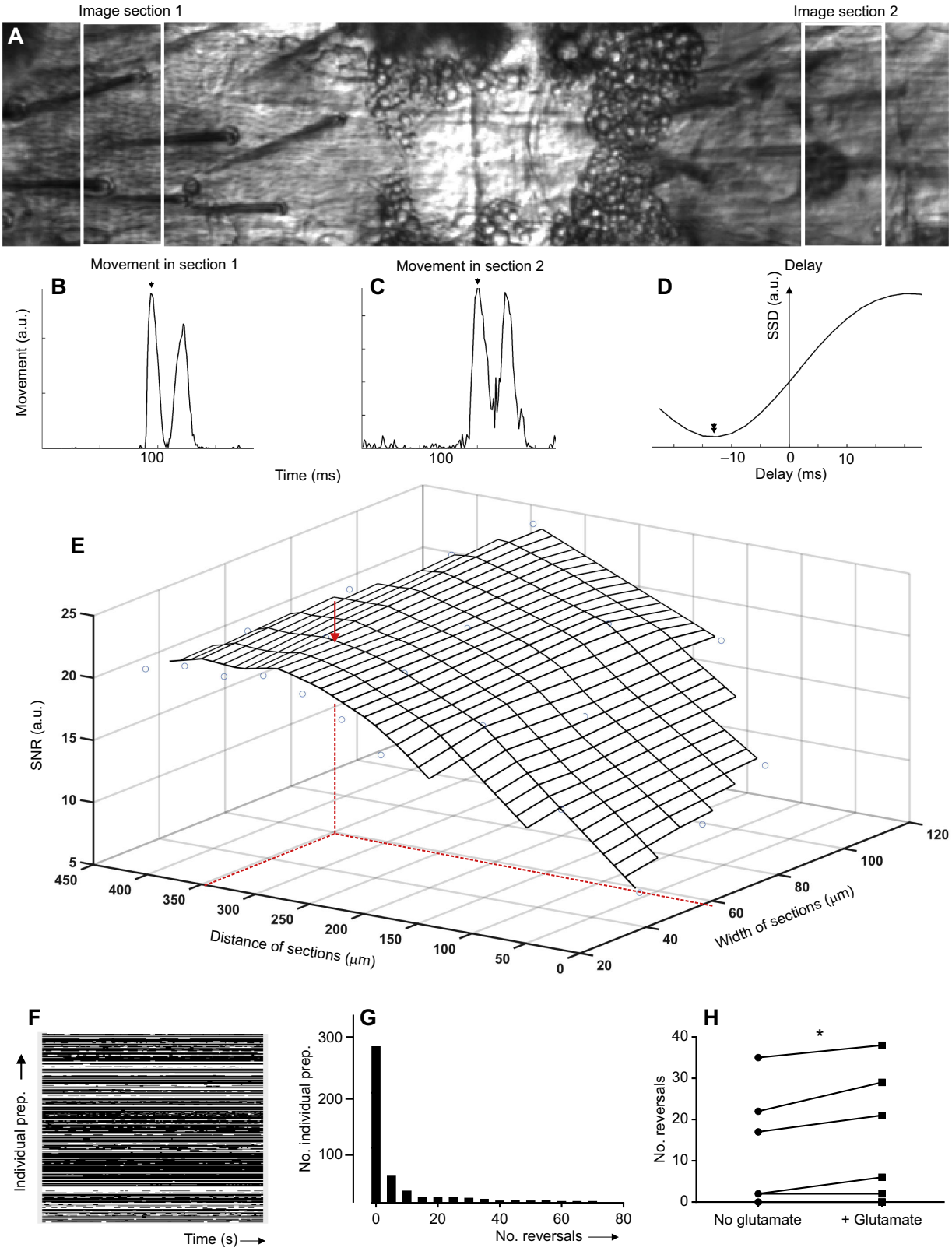

Fig. 2. See next page for legend.

Performance characteristics of the *Drosophila* tubular heart

Cardiac output (CO), i.e. the heart's delivery volume, is one of the major indicators of cardiac performance and is defined as the product of heart rate (f_H) and stroke volume (SV). In contrast to the closed and high-pressure human circulatory system, *Drosophila* features an open system that moves haemolymph along the longitudinal axis of its dorsally located contractile vessel (Wasserthal, 2007). Despite the anatomical differences, the two

Journal of Experimental Biology

Journal of Experimental Biology (2017) 220, 4644-4653 doi:10.1242/jeb.164343

Fig. 2. Peristaltic movement along the heart's longitudinal axis. The OFA provides access to direction and magnitude of movement along the heart's longitudinal axis. (A) Movement was independently determined within two image sections located at opposing ends of the window of observation, and delay between movement in the posterior (B) and anterior section (C) was estimated by means of the sum-of-square difference (SSD, section 1 −section2; D). (E) The distance and width of sections impacted on the signal-to-noise ratio (SNR) of longitudinal movement and were optimized to a width of 60 µm at a distance of 350 µm (red arrow). (F) The direction of longitudinal movement (beat direction), shown as a function of time (*x*-axis) for *N*=400 individual preparations (*y*-axis). Black represents anterior movement; white represents posterior movement. (G) The frequency of changes in the direction of cardiac movement, i.e. heart beat reversals, is shown for *N*=400 individual wild-type preparations. (H) Acute application of 50 mmol l^{-1} glutamate increases the likelihood of heart beat reversal. Data represent means±s.e.m. of *N*=19 biological replicates. Statistical differences are denoted by an asterisk (*P<0.05). a.u., arbitrary units.

hearts serve a similar function, i.e. to deliver a particular volume of circulating fluid per time unit, and hence it appears legitimate to transfer established cardiological indicators to the fly system (Fig. 3A; as previously suggested in Wolf et al., 2006; Ocorr et al., 2007a,b,c; Fink et al., 2009; Cammarato et al., 2015; Klassen et al., 2017).

Towards that goal, we estimated *Drosophila*'s cardiac volume (CV) based on the reconstruction of the heart tube's volume (see Fig. 1B), taking account of the fact that the lumen of the tubular heart is reduced but not completely obscured during systolic contraction in contrast to measurements by optical coherence tomography (OCT; Wolf et al., 2006). This fact is respected by the fractional shortening (FS) of the lumen that we determined as a constant factor of 0.6, as previously described (Fink et al., 2009). Note that FS values might vary slightly between different studies dependent on which reference point was chosen within the heart tube. Thereafter, we estimated the stroke volume (SV) as SV=CV×FS−assuming a constant FS for each position of the heart tube and neglecting back pressure and back flow in the first approximation. Thereby, we estimated *Drosophila*'s CO to be around 211 nl min^{-1}, suggesting that flies exhibit a highly agile cardiac system that circulates about 1/5 of its body mass per minute. This system is powered by a peristaltic wave that propagates at 12 mm s^{-1}, as previously reported (Fink et al., 2009), and thus covers the distance of the tubular heart in about 0.1 s.

Cardiovascular performance is adjustable to meet the changing needs of the body, and *Drosophila* governs these adjustments by means of octopamine (OA), the fly counterpart of mammalian noradrenaline (Collins and Miller, 1977). Similar to the human adrenergic response, stimulation of the fly heart with OA results in a variety of positive cardiotropic effects. First, OA triggers a chronotropic response that significantly accelerates f_H, the major determinant of CO (t_{32}=10.67, P<0.001; Fig. 3B). This effect is mainly due to shortening of the diastolic rest period (t_{32}=6.96, P<0.001; Fig. 3C). Second, OA shortens the systolic interval (SI; t_{32}=3.89, P<0.001; Fig. 3D) owing to collective shortening of the contraction phase (CP; t_{32}=7.58, P<0.001; Fig. 3E) and relaxation phase (RP; t_{32}=4.48, P<0.001; Fig. 3F), thus exhibiting positive inotropic and lusitropic effects, which improve contraction and relaxation properties of the fly myocardium, respectively. Finally, OA mediates a positive dromotropic effect as it increases the speed of the peristaltic wave along the longitudinal axis, suggesting that myocytes exhibit a mechanism to facilitate their coordinated excitability (t_{32}=14.16, P<0.001; Fig. 3G).

Taken together, these data establish the OFA as a robust method to benchmark *Drosophila*'s cardiac performance on the basis of well-established parameters derived from human cardiology. Next, we sought to put the informative value of these parameters to the test by analysing established *Drosophila* models of cardiac dysfunction.

Approaching age- and rhythm-related dysfunction

Cardiac myocytes are distinguished by biological stimulators that facilitate the generation and maintenance of an autonomous rhythm due to a complex interplay between ion pumps and voltage-sensitive channels that, in turn, accomplish a periodic discharge of the membrane potential. During this process, potassium (K^+) channels account for membrane potential repolarization, thereby terminating cardiac action potentials. Dysfunction of K^+ channels like the human ether-a-go-go-related gene (*HERG*) or the *KCNQ1* gene that encode K^+ channels responsible for either the rapid or slow repolarizing currents, *I*Kr and *I*Ks, respectively, is assigned to arrhythmical disorders. In humans, that dysfunction manifests as a prolonged QT interval on the surface electrocardiograms known as long-QT syndrome, and is known to cause sudden cardiac death (Jentsch, 2000). Mutation of the *Drosophila KCNQ1* gene gives rise to a comparable condition that is characterized by prolonged contractions of the dorsal vessel and delayed relaxation of the myocardium (Ocorr et al., 2007c). Intriguingly, arrhythmia becomes worse as flies age (Ocorr et al., 2007b,c), so we employed both models, either ageing or knockdown of *Drosophila*'s KCNQ transcripts, to put the diagnostic value of the OFA method to the test.

Firstly, we compared differently aged wild-type cohorts and noticed a qualitative difference that manifested within the M-mode as a prolonged systolic interval accompanied by a prominent extension of the isometric phase in aged (Fig. 4A) but not young flies (Fig. 4B). Secondly, we noticed that knockdown of KCNQ within a hand>bPAC background prolonged SI but, in contrast to age, this occurred as a result of extension of CP and RP with no impact on the isometric phase (Fig. 4C) when compared with genetic controls that expressed the UAS-bPAC transgene in cardiac myocytes but missed the KCNQ knockdown (KCNQ-KD) construct (Fig. 4D). It is noteworthy that the statistical comparison between animals of a common genotype, i.e. young versus old wild-type or hand>bPAC with versus without KCNQ-KD, reflects the impact of experimental manipulation, while a comparison between different genotypes reflects the different genetic outfits. Thus, the M-mode suggests that loss of KCNQ and ageing impact on different aspects of cardiac performance, prompting us to profile the distinct phases of the cardiac cycle: we report that either manipulation extended the systolic interval (t_{28}=6.07, P<0.01 for ageing and t_{25}=4.72, P<0.01 for KCNQ-KD; Fig. 4E) as a consequence of prolongation of both the CP (t_{28}=3.02, P<0.05 for ageing and t_{25}=5.22 for KCNQ-KD, P<0.01; Fig. 4F) and the RP (t_{28}=9.64, P<0.01 for ageing and t_{25}=5.81, P<0.01 for KCNQ-KD; Fig. 4G). However, only ageing significantly extended the IP (t_{28}=3.10, P<0.05 for ageing and t_{25}=0.82, P>0.05 for KCNQ-KD; Fig. 4H), suggesting that old flies suffer from altered calcium handling as has been previously shown (Lin et al., 2011).

Next, we asked whether OA had the capacity to counterbalance age effects and therefore perfused cardiac preparations with 10^{-6} mol l^{-1} OA (Fig. 4I) or used activation of the photoactive adenylyl cyclase bPAC (Stierl et al., 2011) as a means to increase intracellular cAMP levels, and thereby mimic

Journal of Experimental Biology (2017) 220, 4644-4653 doi:10.1242/jeb.164343

A

Parameter	Mean±s.e.m.	Dimension
Cardiac volume (CV)	3.18±0.4	nl
Fractional shortening (FS)	0.62±0.04	–
Stroke volume (SV)	1.99±0.3	nl
Heart rate (f_H)	1.79±0.1	Hz
Cardiac output (CO)	214.8±9.9	nl min^{-1}
Diastolic interval (DI)	443.9±25.5	ms
Systolic interval (SI)	191.1±2.7	ms
Contraction phase (CP)	88.0±1.65	ms
Isometric phase (IP)	16.3±3.18	ms
Relaxation phase (RP)	96.2±2.3	ms
Velocity (V)	12.0±0.67	mm s^{-1}

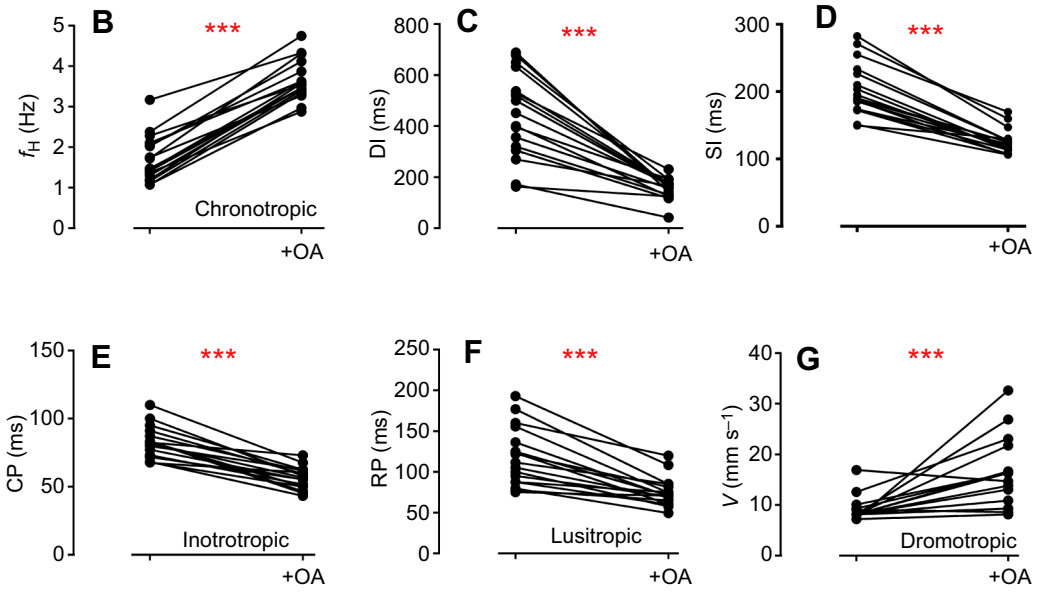

Fig. 3. Characteristic performance of the *Drosophila* heart and its regulation by octopamine. The phenolamine octopamine (OA) exhibits a variety of cardiotropic effects. (A) Adapting established indicators from human cardiology to the fly system allows a detailed and standardized characterization of the fly's cardiovascular performance. (B,C) OA exhibits a variety of cardiotropic effects that impact on particular parameters, i.e. it increases heart rate (B) as a result of shortening of the diastolic interval (C), thus providing a positive chronotropic effect. (D) Application of OA shortens the systolic interval as a result of shortening of the contraction phase (E) and the relaxation phase (F), and thus provides positive inotropic and lusitropic actions, respectively. (G) OA augments movement of the peristaltic wave along the heart's longitudinal axis, thus providing a positive dromotropic effect. Data represent means±s.e.m. of N=30 biological replicates. Statistical differences are denoted by asterisks (***P<0.001).

activation of a G-protein-coupled OA receptor (Fig. 4J). While the pharmacological application of OA compensated for the lack of performance of the aged cohort to levels indistinguishable from those of their young siblings (Fig. 4K–N), the optogenetic approach improved some, but not all, conditions caused by KCNQ knockdown (Fig. 4K–M). Intriguingly, rescue of the positive lusitropic effect was spared, suggesting that shortening of the RP (t_{28}=0.75, P>0.05 for ageing and t_{25}=4.21, P<0.01 for KCNQ-KD; Fig. 4N) requires KCNQ's slow repolarizing current. However, as activation of bPAC and perfusion of OA exhibit different effects on heart rate at early time points (compare Fig. 4I and J), we cannot exclude that differences in RP result from differences in manipulation.

Nevertheless, this analysis ratified OFA as a powerful tool to facilitate a detailed characterization of cardiac conditions. Its discriminative power, however, originates in its unique design to provide a continuous registration of coherent movement, an attribute that we have so far exploited only indirectly. Thus, we tested the possibility that coherent movement in itself might serve as an adequate phenotypic indicator.

The direction of contractile movement aids as a phenotypical indicator

Towards this goal, we used polar coordinates to represent the trajectories of coherent movement magnitude and direction via the radius vector and angle, respectively (Fig. 5A). It should be noted

Journal of Experimental Biology

Journal of Experimental Biology (2017) 220, 4644-4653 doi:10.1242/jeb.164343

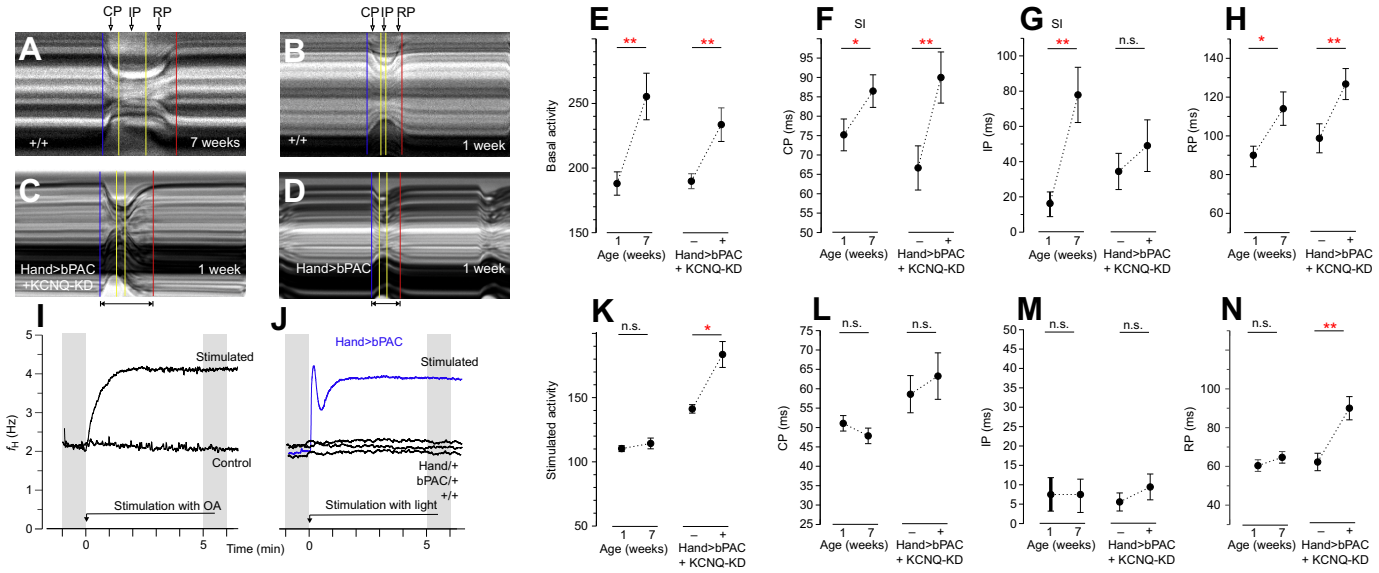

Fig. 4. *Drosophila* models of cardiac dysfunction. The generation and maintenance of a stable cardiac rhythm are affected by age and dysfunction of the KCNQ channel, a slowly repolarizing, voltage-gated potassium channel that terminates the cardiac action potential. While the M-mode visualizes the effects of age (A,B) or KCNQ knockdown (C,D) on the characteristic movement of the cardiac vessel, the OFA provides an in-depth analysis of how particular parameters are changed in either condition (E–N). (E) Age and KCNQ knockdown (KD) similarly prolonged the systolic interval as a result of elongation of the contraction phase (F). In contrast, only age significantly impacts on the isometric phase (G), while the relaxation phase was similarly affected in the two conditions (H). Perfusion of wild-type cardiac preparation with OA stimulated cardiac performance (I) as did light activation of the photoactive cyclase bPAC when expressed within the cardiac vessel (J). Stimulations exhibited different effects on the systolic interval (K), although the contraction phase (L) and the isometric phase (M) were similarly accelerated. (N) In contrast, the relaxation phase was insensitive to light-induced cAMP signals in a KCNQ-KD background. Data represent means±s.e.m. of N=30 biological replicates. Statistical differences are denoted by asterisks (*P<0.05; **P<0.01; n.s., not significant).

that the radius vector is relative to the body axis, i.e. 0 deg represents anterior and 180 deg represents posterior. Plotting the movement of consecutive contractions and relaxations yielded two sets of curves, each exhibiting a high level of consistency and therefore suggesting a stereotyped pattern of coherent movement within a particular preparation. We then averaged the movement of 400 individual preparations and plotted their mean vectors, which appeared to be normally distributed (Fig. 5B). Finally, we introduced the average lead vector to illustrate magnitude and direction of coherent movement during contraction or relaxation of wild-type heart tubes (Fig. 5C).

Next, we probed the informative value of the lead vector as a phenotypic indicator by using Hand-Gal4 (Sellin et al., 2006) to drive expression of a UAS-RNAi transgene within the *Drosophila* heart that targeted the ryanodine receptor (RyR), the major source of intracellular calcium (Fig. 5D). We report that knockdown of RyR minimized the magnitude of coherent movement when compared with genetic controls that bore either transgene alone, but not in combination (Fig. 5D; one-way ANOVA for contraction: $F_{2,59}$=7.59, P<0.05 and for relaxation: $F_{2,59}$=9.42, P<0.01). Moreover, the direction of coherent movement remained unchanged (one-way ANOVA for contraction: $F_{2,59}$=0.20, P=0.81 and for relaxation: $F_{2,59}$=0.52, P=0.12), in line with the recognized function of RyR as a pacesetter of contraction strength (Sullivan et al., 2000). The essence of this phenotype, i.e. a ‘shallow’ contraction, is most suitably illustrated by a video of hand>RyR-KD flies (Movie 2).

We then used a constitutive active form of the GTPase *ras* (UAS-ras^{act}) to induce cardiac hypertrophy and increase myocardium thickness (Yu et al., 2013). Ras-induced hypertrophy increased the magnitude of coherent movement during both contraction and relaxation (Fig. 5E; one-way ANOVA for contraction movement: $F_{2,51}$=21.74, P<0.001 and for relaxation movement: $F_{2,51}$=17.56, P<0.001) but dissociated their directions, with only relaxing movement being significantly changed when compared with genetic controls (Fig. 5E; one-way ANOVA for contraction direction: $F_{2,51}$=0.29, P=0.75 and for relaxation direction: $F_{2,51}$=5.95, P<0.01). Again, the essence of this phenotype, i.e. ‘inclined’ movement, is most suitably illustrated by a video of hand>ras^{act} flies (Movie 3). We speculate that inclined movement is probably due to disarrayed fibres (Fig. 5F,G) that produce lateral force to the heart tube and impact on elastic properties of the tissue by means of increased wall thickness. An alternative source of lateral movement is the allary muscles that hold the heart tube at place within the abdomen and may contribute to a different extent to the net movement in the case of cardiomyopathies.

Altogether, these results establish the lead vector of coherent movement as a suitable indicator of qualitative changes of the heart tube’s beating characteristics. Moreover, these different movement ‘qualities’ do not compromise the OFA’s ability to allocate particular phases of cardiac action to the time line of observation as indicated by the lack of significant changes in RyR knocked down flies when compared with appropriate genetic controls (Fig. 5H–K). Conversely, the OFA manages to reliably detect the lateral movement of hypertrophied hearts and correctly modify appropriate phases of contraction (CP; Fig. 5I) and relaxation (RP; Fig. 5K). Taken together, these results confirm coherent movement in itself as a valuable phenotypic indicator that provides novel information and improves the usefulness of *Drosophila* as a model of cardiac diseases.

DISCUSSION

Diagnosis of a heart condition depends on the availability of a meaningful parameter that reflects the underlying physiological

Journal of Experimental Biology

Journal of Experimental Biology (2017) 220, 4644-4653 doi:10.1242/jeb.164343

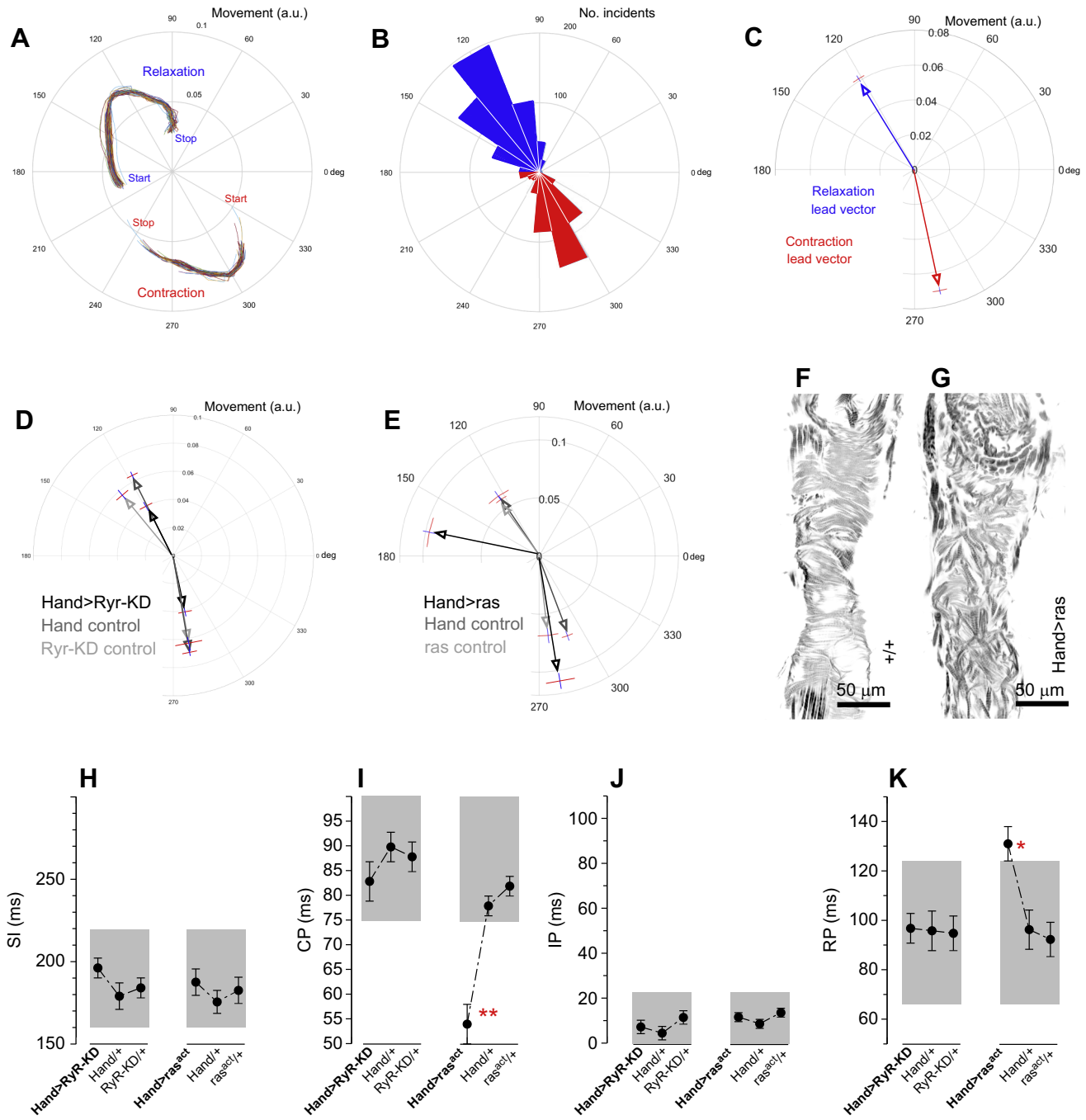

Fig. 5. Coherent movement as a phenotypical indicator. The continuous data on direction and magnitude of movement within the movies of a beating *Drosophila* heart are informative about the performance of the contractile vessel. (A) Movement during consecutive cycles of contraction and relaxation are superimposed and reveal stereotyped movement patterns that can be represented by mean radial vectors. *N*=1. (B) The mean radial vectors of *N*=400 wild-type preparations appear normally distributed. (C) The wild-type average lead vector represents the mean of *N*=400 mean radial vectors. (D) Knockdown of the ryanodin receptor (RyR) diminishes coherent movement, suggesting weakness of the myocardium (*N*>20). (E) Ectopic expression of a constitutively active ras transgene within the heart tube causes cardiac hypertrophy as a result of multiplication of cardiac muscle fibres (*N*>20). (F) Optical section showing a wild-type (+/+) heart contrasted with phalloidin. Scale bar represents 50 µm. (G) Ras-induced hypertrophy as a result of ectopic expression of the constitutively active ras $85D^{V12}$ transgene (Yu et al., 2013). Scale bar represents 50 µm. (H) The systolic interval was not affected by knockdown of RyR or by ectopic expression of ras^{act}. (I) The contraction phase was significantly shortened upon expression of ras^{act}. (J) The isometric phase was unaffected by either transgene. (K) The relaxation phase was elongated within hypertrophied hearts. Grey boxes in H–K indicate the median±s.d. of our w^{1118} reference. Vector data represent means±s.e.m. of at least *N*=20 biological replicates. Statistical differences are denoted by asterisks (*P<0.05; **P<0.01).

process and allows subdivision of functional from dysfunctional conditions. In the case of the fruit fly, diagnosis of its tubular heart is desirable as *Drosophila* represents a sophisticated model to investigate the genetic basis of cardiac conditions (Lin et al., 2011; Ocorr et al., 2007a). This procedure typically extracts the reiterating sequence of contractions and relaxations from a movie of a beating heart; however, it is challenging to automatically and reliably extract this information for a large number of movies and therefore the

originally employed frame brightness algorithm (FBA) was combined with the changing pixel intensity algorithm (CPIA) to aid in accuracy (Cammarato et al., 2015; Fink et al., 2009). The OFA, in contrast, provides a direct measure of the magnitude and direction of the average vector of coherent movement within the movie that yields a good signal-to-noise ratio and provides continuous data on the direction of movement of the heart tube while the temporal resolution is only limited by the sampling rate of the camera, i.e. 5 ms in our case. This enables the OFA to subscript the time course of observation with the reiterating and stereotyped movement patterns of the myocardium. Moreover, the OFA detects and subscribes qualitative differences in cardiac movement by means of the direction and magnitude of the average lead vector, thereby providing the opportunity to standardize the diagnosis of *Drosophila*'s tubular heart.

The average lead vector as a novel phenotypic indicator

Motion perception is the process of inferring the speed and direction of elements in a scene based on visual inputs. Coherent movement or 'global motion' refers to a situation where neighbouring elements change speed and direction in a similar, i.e. a coherent, fashion (Burr and Santoro, 2001). While our brain uses this principle to distinguish visual objects from background (Sargolini et al., 2006), similar tasks can be achieved by machine vision using appropriate computer algorithms (Lucas and Kanade, 1980). We aided these algorithms within the OFA to distinguish the moving *Drosophila* heart from its non-moving background of the body carcass (see Movie 1) and to compute a remarkably precise signal of when coherent movement occurs (see Fig. 1E). Simultaneously, the algorithms provided the direction of coherent movement for every time point (see Fig. 1F), thereby providing access to the direction and magnitude of movement quality that we plotted using polar coordinates (see Fig. 5A). As the OFA was designed without preference for particular directions or minimum amount of movement, it was also suited to detect and subscribe unforeseen phenotypes like 'shallow' or 'inclined' movements (see Movies 2 and 3). As we experienced the movement to be highly stereotypic, we used simple Gaussian averages, but encourage use of more sophisticated statistical methods to further investigate 'movement quality' in the future.

Improved detection of dynamic parameters

Subscribing the time course of observation with particular phases of cardiac movement was based on a heuristic that accounted for midline symmetry of the image section and defined contraction as coherent movement towards the midline while movement away from the midline was defined as relaxation; together with the isometric phase, these events constituted the systole of the *Drosophila* heart, as previously defined (Cammarato et al., 2015; Fink et al., 2009). While the contraction phase and relaxation phase were clearly indicated by the movement magnitude signal (see Fig. 1M), we determined start and endpoints of the isometric phase based on the second derivative of the movement magnitude curve, i.e. its turning points. By that design, the OFA was able to subscribe the characteristic phases of cardiac action without need for predefined time windows and thus holds potential to access an analysis of rhythm by means of more sophisticated mathematical methods in the future.

Conclusions

The OFA represents a derivative of the SOHA method (Cammarato et al., 2015; Fink et al., 2009) that can easily be integrated into its Matlab-based version and can be run in parallel to provide additional information. As raw data are fully compatible with either method, this analysis can even be performed on pre-existing sets of data. The gain in phenotypic information will improve the usefulness of *Drosophila* as a model of cardiac diseases.

Acknowledgements

We are thankful to Mona Storms for excellent technical support.

Competing interests

The authors declare no competing or financial interests.

Author contributions

Conceptualization: M.S.; Methodology: H.M., M.S.; Software: H.M.; Investigation: D.T., E.M., V.R., D.R., M.E.; Resources: S.S., D.R.; Data curation: D.R., M.S.; Writing - original draft: M.S.; Writing - review & editing: M.S.; Visualization: D.H.; Supervision: M.S.

Funding

This work was supported by grant SCHW1410/3-1 from the Deutsche Forschungsgemeinschaft to M.S. and grants from the Bundesministerium fuer Bildung und Forschung (Smartage, 01GQ1420A) to S.S. and E.M.

Data availability

The source code of optical flow detection we used is publicly available at https://github.com/hmoenck/OFAnalysis_supplementary.

Supplementary information

Supplementary information available online at
http://jeb.biologists.org/lookup/doi/10.1242/jeb.164343.supplemental

References

Albrecht, S., Wang, S., Holz, A., Bergter, A. and Paululat, A. (2006). The ADAM metalloprotease Kuzbanian is crucial for proper heart formation in Drosophila melanogaster. *Mech. Dev.* **123**, 372-387.

Brand, A. H. and Perrimon, N. (1993). Targeted gene expression as a means of altering cell fates and generating dominant phenotypes. *Development* **118**, 401-415.

Burr, D. C. and Santoro, L. (2001). Temporal integration of optic flow, measured by contrast and coherence thresholds. *Vision Res.* **41**, 1891-1899.

Cammarato, A., Ocorr, S. and Ocorr, K. (2015). Enhanced assessment of contractile dynamics in Drosophila hearts. *BioTechniques* **58**, 77-80.

Cao, G., Platisa, J., Pieribone, V. A., Raccuglia, D., Kunst, M. and Nitabach, M. N. (2013). Genetically targeted optical electrophysiology in intact neural circuits. *Cell* **154**, 904-913.

Clerico, A., Giannoni, A., Vittorini, S. and Passino, C. (2011). Thirty years of the heart as an endocrine organ: physiological role and clinical utility of cardiac natriuretic hormones. *Am. J. Physiol. Heart Circ. Physiol.* **301**, H12-H20.

Collins, C. and Miller, T. (1977). Studies on the action of biogenic amines on cockroach heart. *J. Exp. Biol.* **67**, 1-15.

Dulcis, D. and Levine, R. B. (2005). Glutamatergic innervation of the heart initiates retrograde contractions in adult Drosophila melanogaster. *J. Neurosci.* **25**, 271-280.

Fink, M., Callol-Massot, C., Chu, A., Ruiz-Lozano, P., Izpisua Belmonte, J. C., Giles, W., Bodmer, R. and Ocorr, K. (2009). A new method for detection and quantification of heartbeat parameters in Drosophila, zebrafish, and embryonic mouse hearts. *BioTechniques* **46**, 101-113.

Gill, S., Le, H. D., Melkani, G. C. and Panda, S. (2015). Time-restricted feeding attenuates age-related cardiac decline in Drosophila. *Science* **347**, 1265-1269.

Gordon, T., Castelli, W. P., Hjortland, M. C., Kannel, W. B. and Dawber, T. R. (1977). Diabetes, blood lipids, and the role of obesity in coronary heart disease risk for women. The Framingham study. *Ann. Intern. Med.* **87**, 393-397.

Guo, A., Li, L., Xia, S. Z., Feng, C. H., Wolf, R. and Heisenberg, M. (1996). Conditioned visual flight orientation in Drosophila: dependence on age, practice, and diet. *Learn. Mem.* **3**, 49-59.

Horn, B. K. P. and Schunck, B. G. (1981). Determining optical flow. *Artificial Intelligence* **17**, 185-203.

Jentsch, T. J. (2000). Neuronal KCNQ potassium channels: physiology and role in disease. *Nat. Rev. Neurosci.* **1**, 21-30.

Johnson, E., Ringo, J., Bray, N. and Dowse, H. (1998). Genetic and pharmacological identification of ion channels central to the Drosophila cardiac pacemaker. *J. Neurogenet.* **12**, 1-24.

Klassen, M. P., Peters, C. J., Zhou, S., Williams, H. H., Jan, L. Y. and Jan, Y. N. (2017). Age-dependent diastolic heart failure in an in vivo Drosophila model. *Elife* **6**, e20851.

Lin, N., Badie, N., Yu, L., Abraham, D., Cheng, H., Bursac, N., Rockman, H. A. and Wolf, M. J. (2011). A method to measure myocardial calcium handling in adult Drosophila. *Circ. Res.* **108**, 1306-1315.

Lo, P. C. H., Skeath, J. B., Gajewski, K., Schulz, R. A. and Frasch, M. (2002). Homeotic genes autonomously specify the anteroposterior subdivision of the Drosophila dorsal vessel into aorta and heart. *Dev. Biol.* **251**, 307-319.

Lucas, B. D. and Kanade, T. (1981). An iterative image registration technique with an application to stereo vision. Proc 7th Intl Joint Conf Artificial Intelligence (IJCAI), pp. 674-679.

Neely, G. G., Kuba, K., Cammarato, A., Isobe, K., Amann, S., Zhang, L., Murata, M., Elmén, L., Gupta, V., Arora, S. et al. (2010). A global in vivo Drosophila RNAi screen identifies NOT3 as a conserved regulator of heart function. *Cell* **141**, 142-153.

Ocorr, K., Akasaka, T. Bodmer, R. (2007a). Age-related cardiac disease model of Drosophila. *Mech. Ageing Dev.* **128**, 112-116.

Ocorr, K., Perrin, L., Lim, H.-Y., Qian, L., Wu, X. and Bodmer, R. (2007b). Genetic control of heart function and aging in Drosophila. *Trends Cardiovasc. Med.* **17**, 177-182.

Ocorr, K., Reeves, N. L., Wessells, R. J., Fink, M., Chen, H.-S. V., Akasaka, T., Yasuda, S., Metzger, J. M., Giles, W., Posakony, J. W. et al. (2007c). KCNQ potassium channel mutations cause cardiac arrhythmias in Drosophila that mimic the effects of aging. *Proc. Natl. Acad. Sci. USA* **104**, 3943-3948.

Ocorr, K., Fink, M., Cammarato, A., Bernstein, S. I. and Bodmer, R. (2009). Semi-automated optical heartbeat analysis of small hearts. *J. Vis. Exp.*, e1435.

Olson, T. M., Kishimoto, N. Y., Whitby, F. G. and Michels, V. V. (2001). Mutations that alter the surface charge of alpha-tropomyosin are associated with dilated cardiomyopathy. *J. Mol. Cell. Cardiol.* **33**, 723-732.

Sargolini, F., Fyhn, M., Hafting, T., McNaughton, B. L., Witter, M. P., Moser, M. B. and Moser, E. I. (2006). Conjunctive representation of position, direction, and velocity in entorhinal cortex. *Science* **312**, 758-762.

Sellin, J., Albrecht, S., Kölsch, V. and Paululat, A. (2006). Dynamics of heart differentiation, visualized utilizing heart enhancer elements of the Drosophila melanogaster bHLH transcription factor Hand. *Gene Expr. Patterns* **6**, 360-375.

Shah, S. H., Kraus, W. E. and Newgard, C. B. (2012). Metabolomic profiling for the identification of novel biomarkers and mechanisms related to common cardiovascular diseases: form and function. *Circulation* **126**, 1110-1120.

Stierl, M., Stumpf, P., Udwari, D., Gueta, R., Hagedorn, R., Losi, A., Gärtner, W., Petereit, L., Efetova, M., Schwarzel, M. et al. (2011). Light modulation of cellular cAMP by a small bacterial photoactivated adenylyl cyclase, bPAC, of the soil bacterium Beggiatoa. *J. Biol. Chem.* **286**, 1181-1188.

Sullivan, K. M. C., Scott, K., Zuker, C. S. and Rubin, G. M. (2000). The ryanodine receptor is essential for larval development in Drosophila melanogaster. *Proc. Natl. Acad. Sci. USA* **97**, 5942-5947.

Ugur, B., Chen, K. and Bellen, H. J. (2016). Drosophila tools and assays for the study of human diseases. *Dis. Model. Mech.* **9**, 235-244.

Wasserthal, L. T. (2007). Drosophila flies combine periodic heartbeat reversal with a circulation in the anterior body mediated by a newly discovered anterior pair of ostial valves and 'venous' channels. *J. Exp. Biol.* **210**, 3707-3719.

Wolf, M. J., Amrein, H., Izatt, J. A., Choma, M. A., Reedy, M. C. and Rockman, H. A. (2006). Drosophila as a model for the identification of genes causing adult human heart disease. *Proc. Natl. Acad. Sci. USA* **103**, 1394-1399.

Yu, L., Daniels, J., Glaser, A. E. and Wolf, M. J. (2013). Raf-mediated cardiac hypertrophy in adult Drosophila. *Dis. Model. Mech.* **6**, 964-976.

Yusuf, S., Reddy, S., Ounpuu, S. and Anand, S. (2001). Global burden of cardiovascular diseases: part I: general considerations, the epidemiologic transition, risk factors, and impact of urbanization. *Circulation* **104**, 2746-2753.

Zheng, G., Joo, J., Ganesh, S. K., Nabel, E. G. and Geller, N. L. (2005). On averaging power for genetic association and linkage studies. *Hum. Hered.* **59**, 14-20.

Zhu, Y. C., Yocom, E., Sifers, J., Uradu, H. and Cooper, R. L. (2016). Modulatory effects on Drosophila larva hearts: room temperature, acute and chronic cold stress. *J. Comp. Physiol. B* **186**, 829-841.

Supplementary Movies

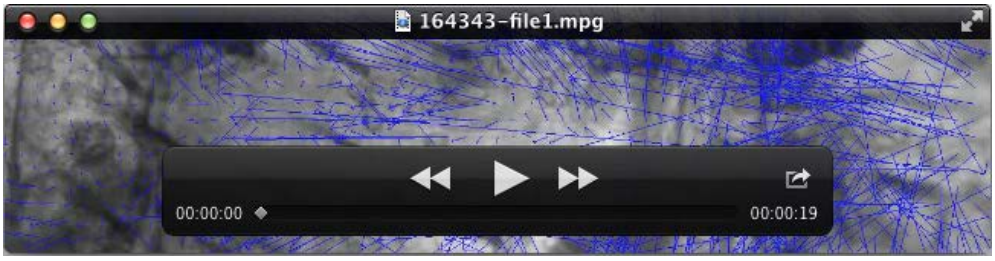

Movie 1: Slow motion video of a beating *Drosophila* heart illustrating coherent movement vectors. Genotype: wild type Canton-S. The original video was captured at 207 fps.

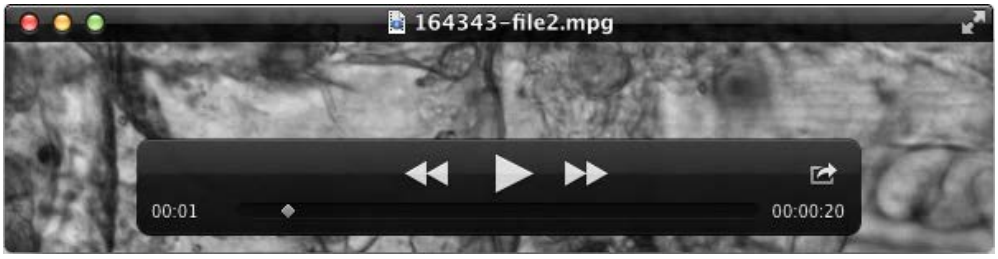

Movie 2: Slow motion video of a beating *Drosophila* heart illustrating "shallow" contractions of a RyR-knocked down heart. Genotype: hand>UAS-RyR-KD. The original video was captured at 207 fps.

Movie 3: Slow motion video of a beating *Drosophila* heart illustrating "inclined" contractions of a hypertrophied heart. Genotype: hand>UAS-Ras85D^{V12}. The original video was captured at 207 fps.

Journal of Experimental Biology • Supplementary information